

PAPER • OPEN ACCESS

Broadband THz Edge-Enhanced Imaging Technology Based on Electro-Optic Sampling

To cite this article: Xingming Yuan *et al* 2023 *J. Phys.: Conf. Ser.* **2525** 012025

View the [article online](#) for updates and enhancements.

You may also like

- [Facial identification in very low-resolution images simulating prosthetic vision](#)
M H Chang, H S Kim, J H Shin et al.

- [Application of Walsh filters and subsequent angular-stitching for edge enhancement](#)
Joydeep Chatterjee, Semanti Chakraborty and Kanik Palodhi

- [Tunable edge enhancement by higher-order spiral Fresnel incoherent correlation holography system](#)
Yuanzhuang Bu, Xi Wang, Yu Li et al.

ECS
The
Electrochemical
Society
Advancing solid state &
electrochemical science & technology

DISCOVER
how sustainability
intersects with
electrochemistry & solid
state science research

Broadband THz Edge-Enhanced Imaging Technology Based on Electro-Optic Sampling

Xingming Yuan², Ying Li^{2,a}, Qinggang Lin¹, Jiapin Chen¹, Yi Cai^{1,*}, Shixiang Xu¹, Jingzhen Li¹

¹Shenzhen Key Laboratory of Micro-Nano Photonic Information Technology, Key Laboratory of Optoelectronic Devices and Systems of Ministry of Education and Guangdong Province, College of Physics and Optoelectronic Engineering, Shenzhen University, Guangdong 518060, China

²SZU-NUS Collaborative Innovation Center for Optoelectronic Science & Technology, Key Laboratory of Optoelectronic Devices and Systems of Ministry of Education and Guangdong Province, Shenzhen University, Guangdong 518060, China

^aEmail: queenly@vip.sina.com

*Email: Caiyi@szu.edu.cn

Abstract. Based on the radial Hilbert transform of spatial filtering and electro-optical sampling, we propose a broadband terahertz edge-enhanced imaging method in this work. Instead of using a narrow-band THz vortex phase plate, here we use vortex ultrashort laser pulse to realize the THz enhancement imaging which can be applied for few-cycle THz imaging. The principle of edge enhancement is analyzed theoretically, and the analytical expression of the final terahertz imaging is derived. We found that edge-enhancement imaging corresponds to the nonlinear term of the THz field, and the background and linear terms can be suppressed when the static birefringent phase is set to zero. The simulations show that our method can effectively improve the contrast and signal-to-noise ratio of terahertz imaging.

1. Introduction

Terahertz imaging ^[1] has excellent application prospects in biomedical diagnosis ^[2-3], non-destructive testing ^[4-5], structural analysis ^[6-7], and other fields. However, the traditional terahertz imaging method has the problem of low imaging contrast. When imaging an object with low contrast amplitude or phase, the scattering information of these defective details is easily covered by a strong background, since the edge details or hidden defects are much smaller than the overall structure. In the frequency domain, this important information corresponds to high-frequency components, which will decay exponentially with the increase of propagation distance. Therefore, such a typical imaging method cannot obtain terahertz images with ideal contrast, which makes edge detection and feature recognition ^[8-12] in subsequent image processing complex.

To improve the imaging quality, Fitzgerald et al. ^[13] made an early attempt to enhance the contrast of terahertz images in 2001 and proposed a terahertz dark-field imaging based on electro-optical sampling, which enhances the image contrast by analyzing the scattering and diffraction characteristics. In recent years, spatial filtering imaging technology has attracted much attention. Its application in imaging systems can achieve considerable imaging contrast and has made significant research achievements in visible and infrared bands ^[14-17]. This technology originates from the Hilbert transform, which can



selectively enhance the edge of the input image to make it have the effect of stereo relief. With the edge distribution density increase, the impact of stereo relief is more significant. Therefore, it is also called edge enhancement imaging, which is an essential optical information processing technology. In 2000, Davis et al. [18] proposed the radial Hilbert transform and applied it to image processing, which can obtain isotropic two-dimensional edge enhancement, opening up a new research field for two-dimensional image information processing. This technology is widely used in optical microscopes [19-20], medical imaging [21], and other fields, and is an essential and convenient image-processing method.

Based on the classic 4f system, Liu et al. [22] proposed a terahertz vortex spatial filtering imaging method that realized image contrast enhancement by inserting a terahertz vortex device into the Fourier plane. However, this method is only ideal for continuous wave (CW) THz imaging. The bandwidth of terahertz vortex devices is narrow. Therefore, it is unsuitable for broadband terahertz imaging systems. The terahertz imaging system [23-25] based on the terahertz time-domain spectrum system uses electro-optic sampling [26-27] mode, and the direct use of terahertz vortex devices will change the spatial distribution of the terahertz field. Thus changing the spatial distribution of the modulation phase in the electro-optic crystal, results in the loss of essential information in the vicinity of the output image center, and no apparent edge detail enhancement. Therefore, developing a broadband terahertz edge-enhanced imaging method is of excellent significance based on electro-optic sampling.

In this paper, we propose a broadband terahertz edge-enhanced imaging method based on electro-optical sampling which can effectively reduce the imaging contrast and signal-to-noise ratio (SNR) of contrast amplitude or phase objects. This method is a radial Hilbert transform based on spatial filtering, inheriting the advantages of traditional terahertz imaging and spatial filtering imaging, and is an effective method to achieve terahertz high contrast imaging. In our work, the basic principle of terahertz edge enhancement is analyzed theoretically. Furthermore, the edge enhancement results under different conditions are simulated. According to our results of the simulation, the proposed terahertz edge enhancement imaging method can effectively improve image contrast and signal-to-noise ratio.

2. Theoretical analysis

The schematic diagram of our THz edge-enhanced imaging system based on the THz time-domain spectroscopy system is shown in Figure 1. In this system, the pump detection mode is adopted, and the detection crystal is located on the Fourier plane of the input image, which determines that the terahertz vortex device cannot be used. Therefore, we introduce the vortex phase into the detection light to enhance the edge of the terahertz image.

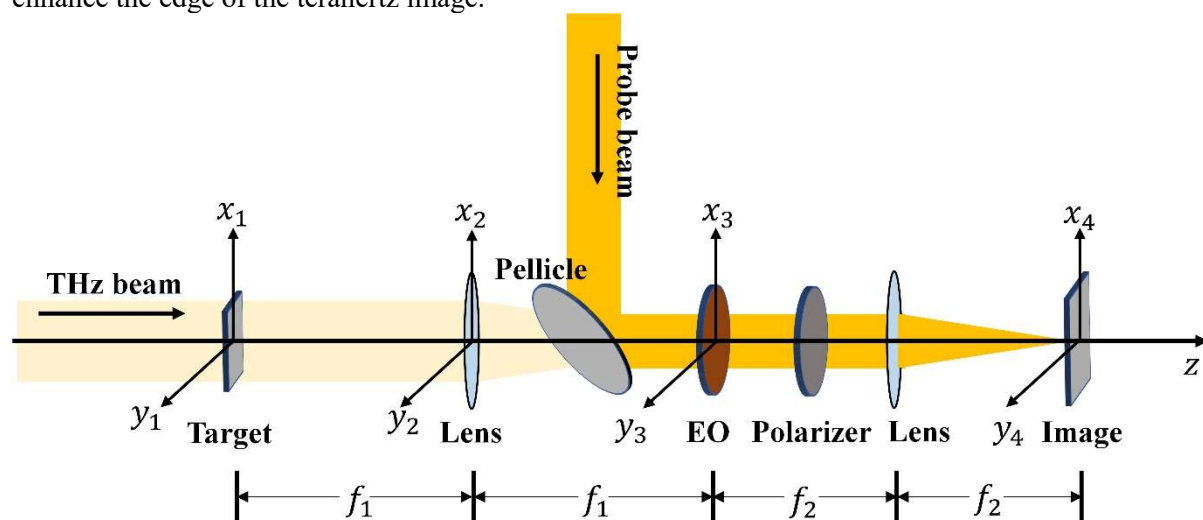


Figure 1. Schematic diagram of broadband terahertz edge-enhanced imaging system based on electro-optical sampling.

Firstly, let's review the basic principle of the Hilbert transform. This is defined in a 4f system. By applying a vortex phase filter to the Fourier spectral plane of the object $E_1(x_1, y_1)$, the Fourier transform of the input image is multiplied by a Hilbert transform mask function $H_m(\rho, \theta)$ to obtain the modulated output image $E_3(x_3, y_3)$, that is

$$E_3(x_3, y_3) = IFT \{ FT \{ E_1(x_1, y_1) \} H_m(\rho, \theta) \} \quad (1)$$

Here $FT \{ \}$ is the Fourier transform and $IFT \{ \}$ is the inverse Fourier transform. $|E_3(x_3, y_3)|^2$ represents the output edge-enhanced image when $H_m(\rho, \theta) \sim H_m(\rho)e^{im\theta}$ carries a vortex phase, where ρ is the radius and θ is the azimuth, and m is a non-zero integer.

In our system, the input image is illuminated by a collimated terahertz beam, and the terahertz electric field $E_1(x_1, y_1)$ passing through the target can be obtained. On the Fourier plane, that is, at the detection crystal, the birefringence phase induced by the terahertz electric field modulates the detection light. The birefringence phase $\Gamma(\rho, \theta)$ is proportional to the terahertz electric field $FT \{ E_1(x_1, y_1) \}$, and it can be expressed as (take [110] ZnTe as an example) [28]

$$\Gamma = \frac{2\pi d}{\lambda} n^3 \gamma_{41} FT \{ E_1(x_1, y_1) \} \quad (2)$$

The spatial distribution of the THz modulation phase corresponds to the spatial distribution of the THz electric field, where λ is the wavelength of the incident light, d is the crystal thickness, n is the refractive index, and γ_{41} is the electro-optic coefficient. When a detection light E_{probe} passes through the detection crystal, the output light field $\tilde{E}_2(x_2, y_2)$ can be expressed as

$$\tilde{E}_2(x_2, y_2) = E_{probe} \sin \left[\frac{\Gamma + \Gamma_0}{2} \right] e^{-\frac{\pi}{4}} \quad (3)$$

Here, the probe light is a vortex light and can be expressed as the product of a circular domain function or Gaussian function with a vortex phase. Among them, the static birefringent phase Γ_0 introduced by an electro-optic crystal is the birefringent phase induced by a terahertz electric field. It can be compensated by a phase compensator. This modulation phase Γ is tiny and can be approximated as follows, namely $\sin \Gamma \sim \Gamma$, $\cos \Gamma \sim 1$. Therefore, Equation (3) can be further expressed as

$$\tilde{E}_2(x_2, y_2) = E_{probe} \left(\sin \Gamma_0 + \frac{\Gamma}{2} \cos \Gamma_0 \right) \quad (4)$$

Then, the output light field is obtained through an inverse Fourier transform

$$\begin{aligned} E_3(x_3, y_3) &= IFT \left\{ \tilde{E}_2(x_2, y_2) \right\} \\ &= \sin \Gamma_0 IFT \{ E_{probe} \} + \frac{1}{2} \cos \Gamma_0 IFT \{ E_{probe} \Gamma \} \end{aligned} \quad (5)$$

Where $IFT \{ \}$ is the inverse Fourier transform. Therefore, the light intensity recorded by the array detector of the output light field can be obtained

$$\begin{aligned}
I &= |E_3(x_3, y_3)|^2 \\
&= \frac{1}{4} \cos^2 \Gamma_0 \left| IFT \{ E_{probe} \Gamma \} \right|^2 + \sin^2 \Gamma_0 \left| IFT \{ E_{probe} \} \right|^2 \\
&\quad + \frac{1}{2} \sin(2\Gamma_0) \left| IFT \{ E_{probe} \} IFT \{ E_{probe} \Gamma \} \right| \cos \Delta \varphi \\
&= I_{IM} + I_B + I_L
\end{aligned} \tag{6}$$

In traditional terahertz electro-optic sampling, the first item is the nonlinear term (containing the quadratic of Γ), leading to signal distortion. The second item is the background item, which can be eliminated by balance detection; The third term is the linear term of the terahertz field, which is the signal we need. However, in terahertz edge-enhanced imaging, we need to consider the distribution of the spatial image. In Equation (5), $IFT \{ E_{probe} \}$ represents the focus field of the probe light, which is spatially distributed in a small area near the center, which corresponds to the second and third terms of Equation (6). In the first term of Equation (6), the factor Γ is the Fourier transform of THz image meanwhile E_{probe} containing a vortex phase, which is similar to Equation (1). Therefore, the first term presents edge-enhanced images. Both the second and the third terms are proportional to $\sin(\Gamma_0)$ while the first term is proportional to $\cos(\Gamma_0)$, thus, to restrain the background and the linear terms, Γ_0 can be chosen towards 0.

3. Simulation

To achieve terahertz edge-enhanced imaging based on electro-optical sampling, the vortex phase needs to be introduced into the detection light. According to different forms of $H_m(\rho)$, there are three common forms of the probe laser field: circle domain (CD) mode, Laguerre-Gaussian mode (LG), and Bessel-Gaussian mode (BG)[29], i.e.

$$E_{probe} = circ\left(\frac{\rho}{R}\right) \exp(im\theta) \tag{7}$$

$$E_{probe} = \frac{\rho}{\omega} \exp\left(-\frac{\rho^2}{\omega^2}\right) circ\left(\frac{\rho}{R}\right) \exp(im\theta) \tag{8}$$

$$E_{probe} = besselj(n, k) \exp\left(-\frac{\rho^2}{R^2}\right) circ\left(\frac{\rho}{R}\right) \exp(im\theta) \tag{9}$$

Where, R is the detection light radius, m is the vortex order, ω is the parameter to control the maximum position of the point spread function of the LG vortex filter system, n is the Bessel order, and k is the constant related to R and ρ . As shown in Figure 2, we selected a circular object with 100% transmittance in the central area and 0 for the background transmittance as the target. We used the three detection light modes of Equations (7) - (9) for edge enhancement imaging, and we can get the edge enhancement results as shown in Figure 2(b)-(d). (Here, $\omega = 5\rho/R$, $R = 5mm$, $m = 1$.) The results show that the energy of the target image after edge enhancement is concentrated on the edge, and the energy in the circular area is suppressed. To compare the boundaries of each image, the intensity-radius distribution is shown in Figure 2(e), and the curves Target, CD, LG, and BG correspond to (a) - (d), respectively. The simulation shows that our scheme based on electro-optic sampling probed by a vortex laser can realize THz edge-enhanced image. For the CD mode, the edge has an apparent oscillation noise. The LG and BG modes can solve the noise problem and achieve a better edge enhancement effect.

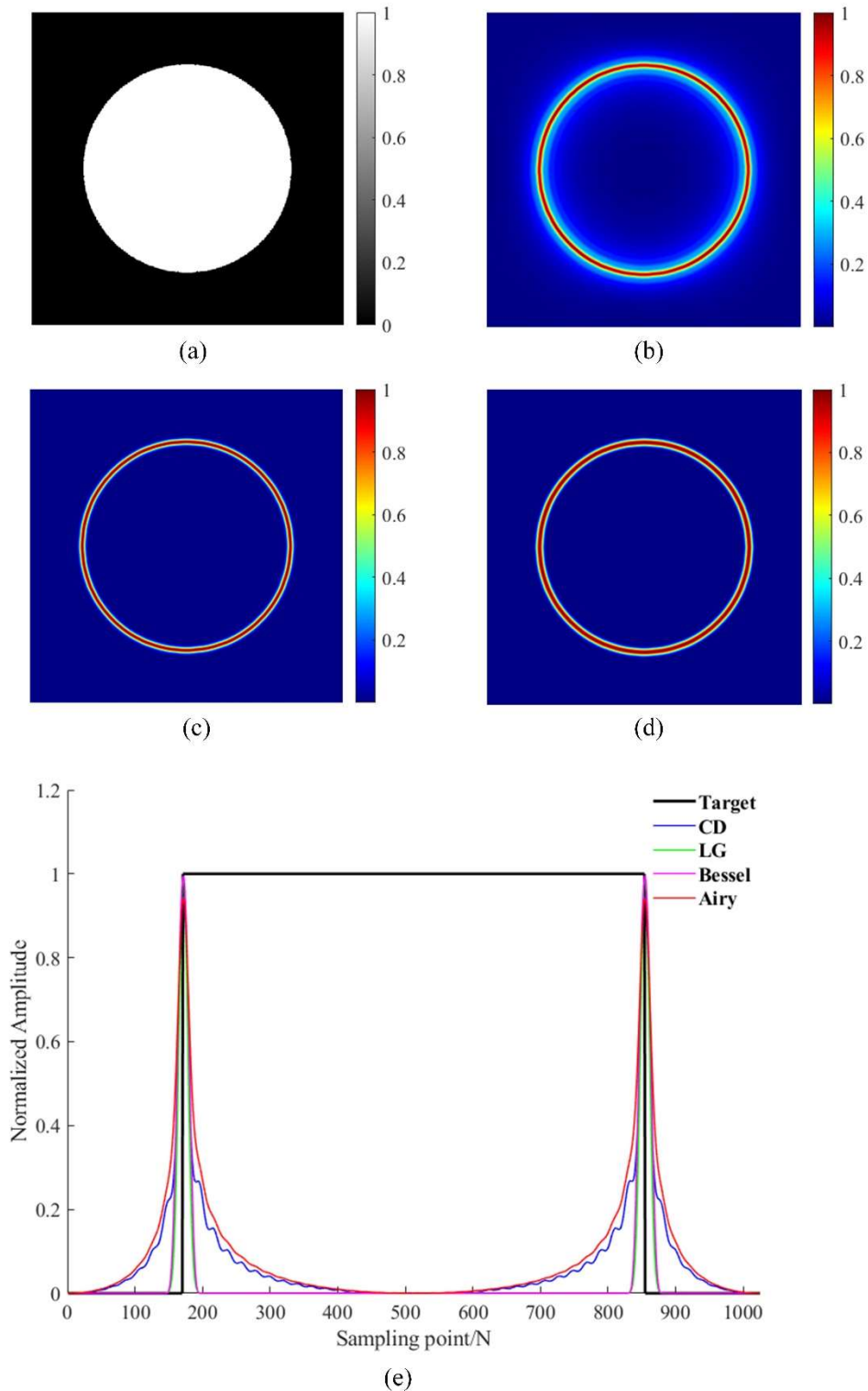


Figure 2. Simulation of edge-enhanced imaging results of a circular target. (a) Circular target with 100% transmittance and 0 background transmittance. (b) Edge-enhanced imaging results in CD mode. (c) Edge-enhanced imaging results in LG mode. (d) Edge enhancement results in BG mode. (e) Section strength distribution curve.

When we choose $\Gamma_0 > 0$, according to Equation (6), the detected light intensity distribution includes the edge enhancement term, background term, and linear term of the terahertz field. As shown in Figure 3, edge enhancement is performed on the "SZU" shaped target image with 100% transmittance and 0 background transmittance, and the light intensity distribution of the edge enhancement term, background term, and linear term of terahertz field corresponding to Figures 3(b)-(d) can be obtained respectively. However, in the actual detected light intensity distribution, the three terms are superposed, as shown in Figure 3(e). The edge-enhanced image for Γ_0 decreases from 0 to 0.0005 is shown in Figures 4(a)-(f). The noise by the background and the linear terms located at the central area of the pictures get weak as Γ_0 decreases. When $\Gamma_0 = 0$, the noise is completely suppressed, just like we analyze above in the Theoretical Analysis part.

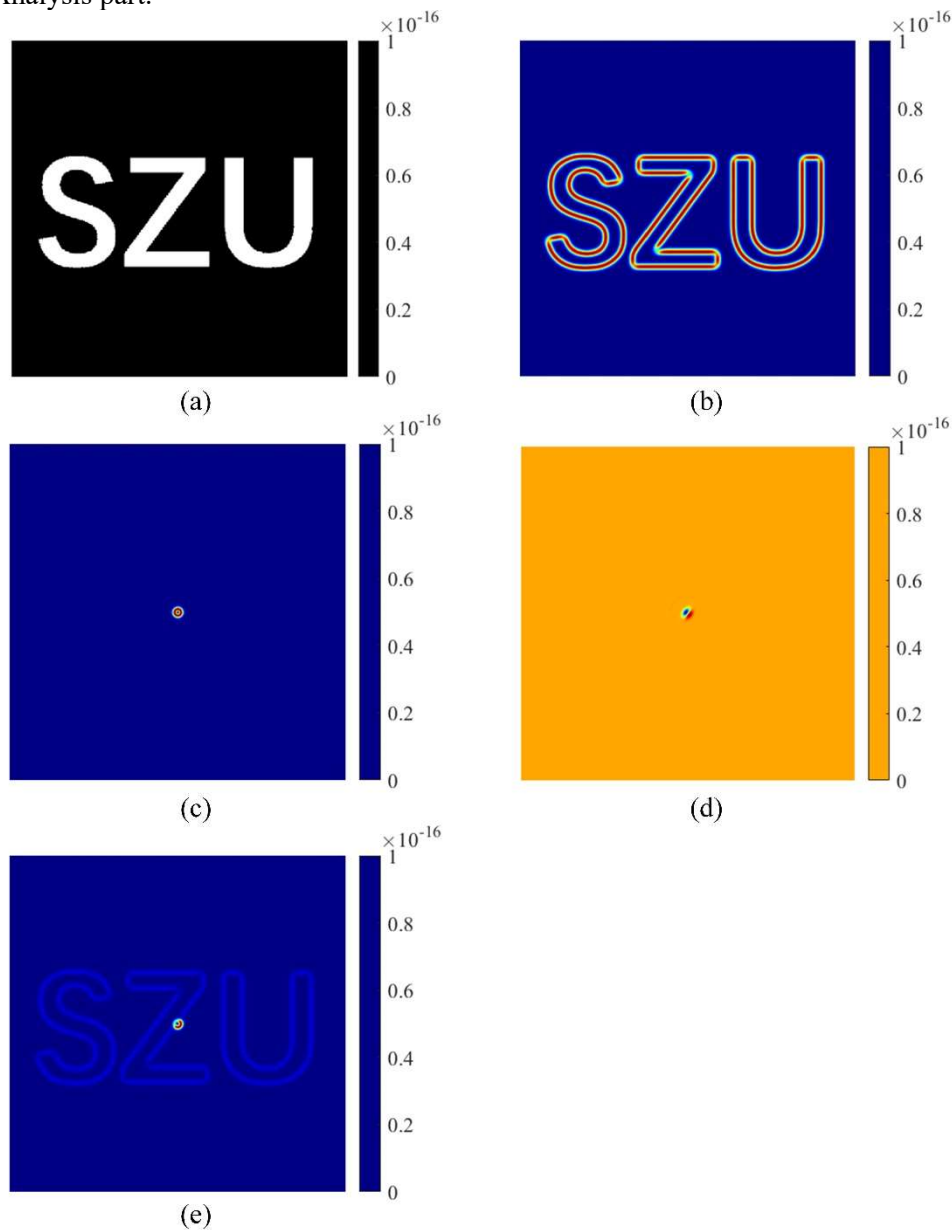


Figure 3. Edge-enhanced imaging results in LG mode. (a) Target object with 100% transmittance and 0 background transmittance. (b) Edge Additions. (c) Background item. (d) Linear term of terahertz field. (e) Superimposed light intensity distribution.

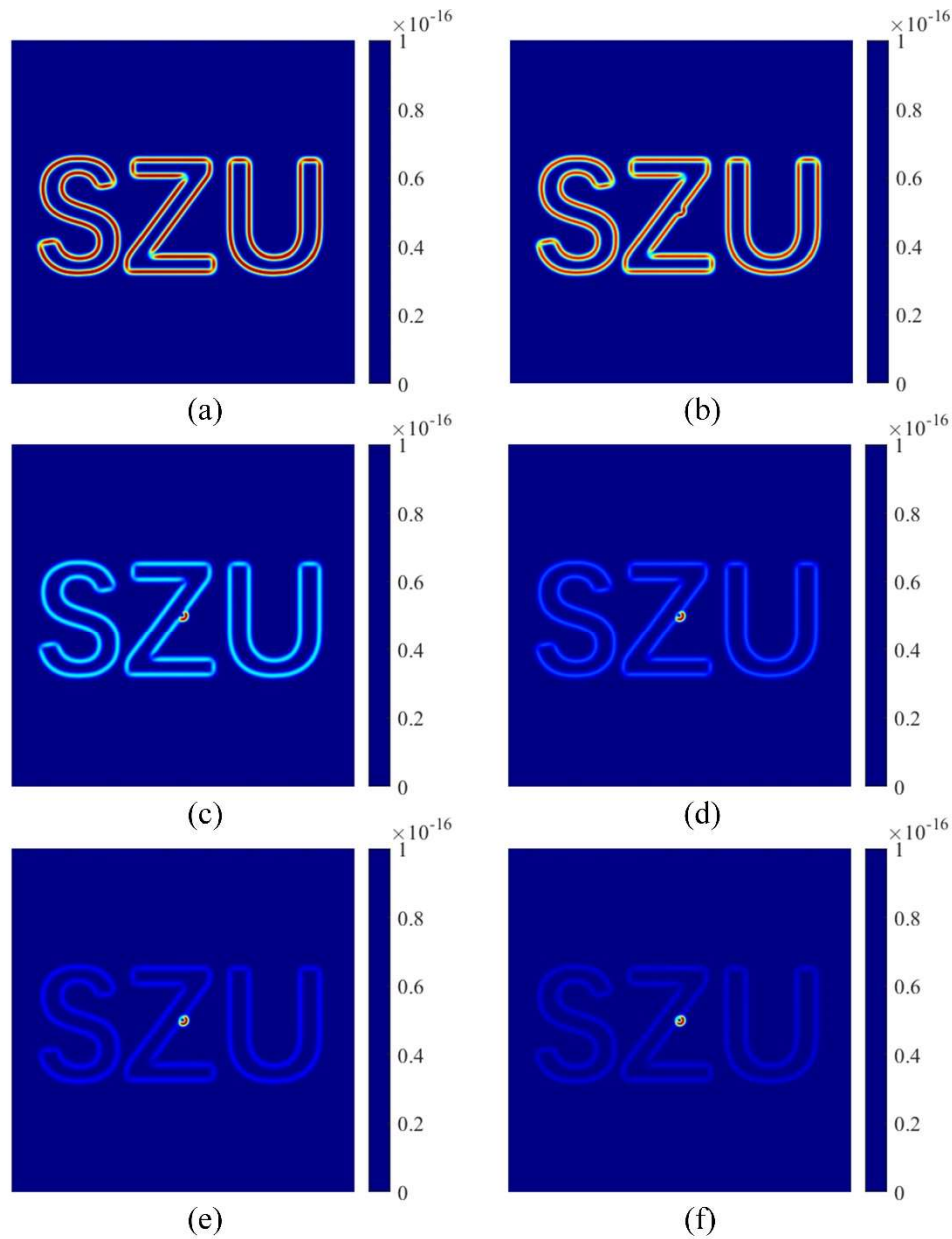


Figure 4. Superimposed light intensity distribution in LG mode. (a) $\Gamma=0.05$, $\Gamma_0=0$. (b) $\Gamma=0.05$, $\Gamma_0=0.0001$. (c) $\Gamma=0.05$, $\Gamma_0=0.0002$. (d) $\Gamma=0.05$, $\Gamma_0=0.0003$. (e) $\Gamma=0.05$, $\Gamma_0=0.0004$. (f) $\Gamma=0.05$, $\Gamma_0=0.0005$.

To show the capability of our scheme to improve the SNR, we use targets with different noise levels, set the probe light to LG mode, and set $\Gamma=0.05$, $\Gamma_0=0$. The results are shown in Figure 5. Figures 5(a), (c), (e), and (g) show the target with the noise means of 0, 1, 0.1, 0.01, and the corresponding edge-enhanced images are shown in Figures 5(b), (d), (f), (h) respectively. The results show that both contrast and SNR are improved.

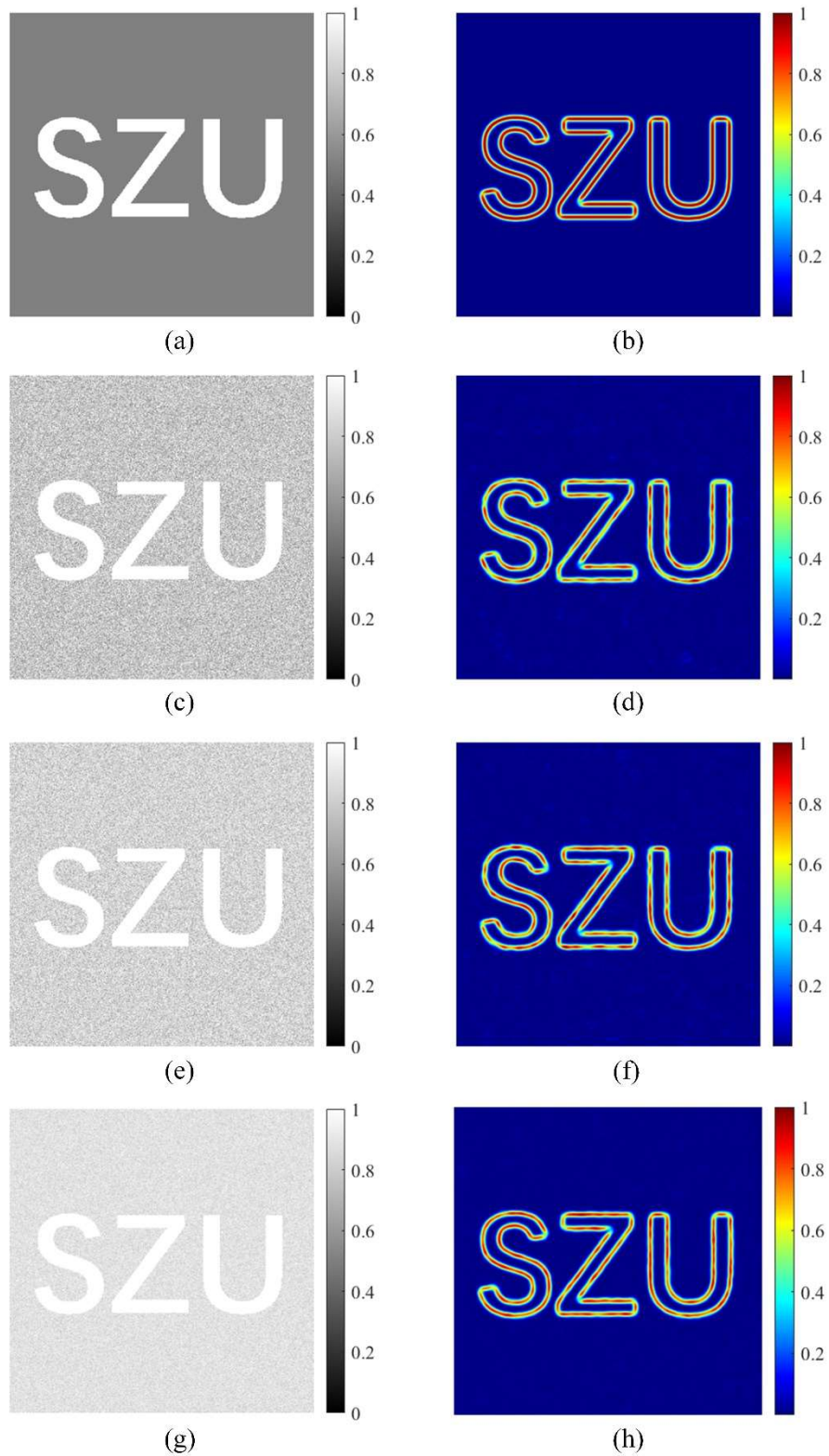


Figure 5. Edge enhancement results under different noises. (a) For images with 100% transmittance and 50% background transmittance, (b) is the edge-enhancement result of (a). (c), (e) and (g) are the Gaussian noise images with the mean value of 0 and the mean values of 1, 0.1, and 0.01 respectively, and (d), (f) and (h) are the corresponding edge-enhancement results.

Above, we have verified that the proposed method can effectively improve the image contrast and SNR of low-contrast amplitude objects. To clarify whether the form has the same edge-enhancement effect on complex pure-phase objects, we conduct the following simulation. Figure 6(a) is the pure-phase object to be measured that we selected. Edge enhancement is achieved in vortex phase filtering, spatial filtering with LG, and spatial filtering with BG, respectively, and the output results in Figures 6(b)-(d) are obtained. From the simulation results, we can see that we can still get a good edge enhancement effect and effectively improve the image contrast.

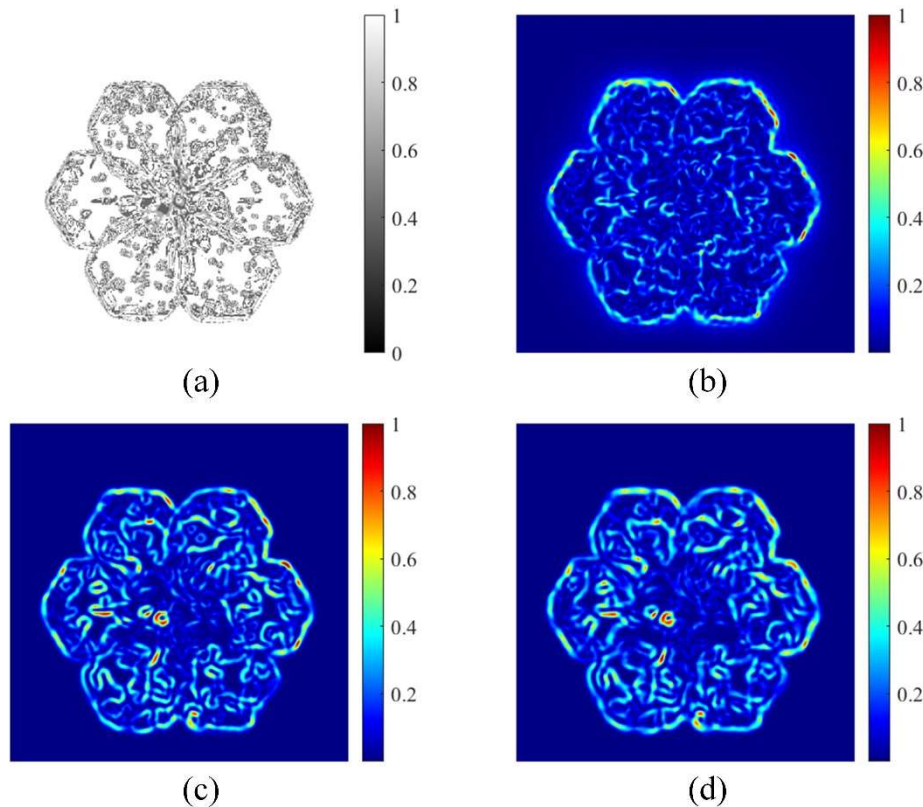


Figure 6. Edge enhancement results of the phase-only object. Figure (a) is a pure phase object, and (b) - (d) is the edge-enhancement results in CD mode, LG mode, and BG mode respectively.

4. Conclusion

In this paper, we propose a wide-band terahertz edge-enhanced imaging method based on the principle of radial Hilbert transform and electro-optical sampling. We theoretically studied the feasibility of this method and calculated the image edge-enhancement effect under different probe light modes and different levels of noise when the vortex order is applied. From the simulated results, it can be seen that the edge-enhanced image has a three-dimensional relief effect, which can effectively improve the imaging contrast and SNR. This work is practical and significant for image information processing and image resolution improvement in the terahertz band.

Acknowledgments

This work is partially supported by the National Natural Science Foundation of China (12174264, 92050203, 62075138, 62275163); Natural Science Foundation of Guangdong Province (2022A1515011457, 2020A1515010541); Shenzhen Fundamental Research Program (JCYJ202001091056064 26, JCYJ2019 0808164007485, JCYJ202103240952130 37, JCYJ20190808121817100, JCYJ20190808143419622, and JCYJ20190808115601653).

References

- [1] Castro-Camus E, Koch M, and Mittleman D M 2022 *Appl. Phys. B-Lasers Optics*. **128**
- [2] Y Y Zhang, C T Wang, B X Huai, S Y Wang, Y T Zhang, D Y Wang, Lrong and Y C Zheng 2021 *Appl. Sci-Basel*. **11**
- [3] Z Y Yan, L G Zhu, K Meng, W X Huang and Q W Shi 2022 *Trends Biotechnol.* **40** 816-30
- [4] Destic F and Bouvet C 2016 *Case Studies in Nondestructive Testing and Evaluation*. **6** 53-62
- [5] Catapano I, Soldovieri L, Mazzola L and Toscano C 2017 *J. Infrared Millim TE*. **38** 1264-77
- [6] Stübling E M, Rehn A, Siebrecht T, Bauckhage Y, Öhrström L, Eppenberger P, Balzer J C, Rühli F and Koch M 2019 *Sci. Rep.* **9** 3390
- [7] Amirkhan F, Sakata R, Takiguchi K, Arikawa T, Ozaki T, Tanaka K and Blanchard F 2019 *J. Opt. Soc. Am. B*. **36** 2593-601
- [8] Chapdelaine Q, Nallappan K, Cao Y, Guerboukha H, Chernomyrdin N, Zaytsev K and Skorobogatiy M 2022 *Opt. Mater. Express*. **12** 3015-31
- [9] Xiong H T, Cai J H, Zhang W H, Hu J S, Deng Y X, Miao J G, Tan Z Y, Li H, Cao J C and Wu X J 2021 *iScience*. **24** 103316
- [10] Wang J R, Lindley-Hatcher H, Liu K, and Pickwell-MacPherson E 2020 *Biomed. Opt. Express*. **11** 4484-90
- [11] Lee G, Lee J, Park Q H and Seo M 2022 *ACS Photonics*. **9** 1500-12
- [12] Chen H, Zhang Y, Li X, Chen X F, Ma S H, Wu X M, Qiu T Z, and Zhang W F 2019 *J. INFRARED MILLIM TE*. **40** 456-65
- [13] Löffler T, Bauer T, Siebert K J, Roskos H G, Fitzgerald A and Czasch S 2001 *Opt. Express*. **9** 616-21
- [14] Liu L, Wang H Y, Ning Y, Guo C and Ren G 2019 *Laser Phy.* **29** 015401
- [15] Wang Y Q, Fang J N, Zheng T T, Liang Y, Hao Q, Wu E, Yan M, Huang K, and Zeng H P 2021 *Laser & Photonics Reviews*. **15** 2100189
- [16] Wang J K, Zhang W H, Qi Q Q, Zheng S S and Chen L X 2015 *Scientific Reports*. **5** 15826
- [17] Wang H H, Ma J, Yang Z X, Du H R, Kang X W, Su H Z, Gao L and Zhang Z 2022 *Frontiers in Physics*. **10**
- [18] Davis J A, McNamara D E, Cottrell D M, and Campos J 2000 *Opt. Lett.* **25** 99-101
- [19] Fürhapter S, Jesacher A, Bernet S and Ritsch-Marte M 2005 *Opt. Express*. **13** 689-94
- [20] Zhao M T, Liang X Z, Li J S, Xie M Y, Zheng H D, Zhong Y C, Yu J H, Zhang J, Chen Z, and Zhu W G 2022 *Laser & Photonics Reviews*. **16** 2200230
- [21] Vidyarthi A 2021 *Biomedical Engineering*. **66** 201-8
- [22] Liu H, Wu S Y, Zhao M, Li C, Liu X J and Fang G Y 2021 *Appl. Sci.* **11** 10
- [23] Xu Y and Jiang X L 2022 *Infrared Physics & Technology*. **127** 104467
- [24] Wang Q, Xie L J and Ying Y B 2022 *Appl. Spectrosc. Rev.* **57** 249-64
- [25] Zanotto L, Piccoli R, Dong J, Caraffini D, Morandotti R and Razzari L 2020 *Opt. Express*. **28** 3795-802
- [26] Jiang Z P, Sun F G, Chen Q, and Zhang X C 199 *Appl. Phys. Lett.* **74** 1191-3
- [27] Winnewisser C, Jepsen P U, Schall M, Schyja V and Helm H 1997 *Appl. Phys. Lett.* **70** 3069-71
- [28] Brunner F D J, Johnson J A, Grübel S, Ferrer A, Johnson S L and Feurer T 2014 *J. Opt. Soc. Am.* **31** 904-10
- [29] Guo C S, Han Y J, Xu J B, and Ding J P 2006 *Opt. Lett.* **31** 1394-6